Chimera States in Continuous Media: Existence and Distinctness

Zachary G. Nicolaou, Hermann Riecke, and Adilson E. Motter

Phys. Rev. Lett. **119**, 244101 — Published 13 December 2017

DOI: 10.1103/PhysRevLett.119.244101

Chimera States in Continuous Media: Existence and Distinctness

Zachary G. Nicolaou,[1] Hermann Riecke,[2,3] and Adilson E. Motter[1,3]

[1] *Department of Physics and Astronomy, Northwestern University, Evanston, IL 60208, USA*
[2] *Department of Engineering Sciences and Applied Mathematics, Northwestern University, Evanston, IL 60208, USA*
[3] *Northwestern Institute on Complex Systems, Northwestern University, Evanston, IL 60208, USA*

The defining property of chimera states is the coexistence of coherent and incoherent domains in symmetric coupled systems. The recent realization that such states might be common in oscillator networks raises the question of whether an analogous phenomenon can occur in continuous media. Here, we show that chimera states can exist in continuous systems even when the coupling is strictly local, as in many fluid and pattern forming media. Using the complex Ginzburg-Landau equation as a model system, we characterize chimera states consisting of a coherent domain of a frozen spiral structure and an incoherent domain of amplitude turbulence. We show that in this case, in contrast with discrete network systems, fluctuations in the local coupling field play a crucial role in limiting the coherent regions. We suggest these findings shed light on new possible forms of coexisting of order and disorder in fluid systems.

Chimera states are spatiotemporal patterns resulting from symmetry breaking. The discovery of such states in oscillator networks demonstrated that even in systems of identically-coupled identical oscillators, mutually synchronized oscillators can coexist with desynchronized ones [1]. This coexistence is particularly remarkable because the coherent and incoherent domains are bidirectionally coupled: it is counterintuitive that the state would be persistent despite the perturbations that desynchronized oscillators unavoidably exert on synchronized ones, and vice versa. Chimera states were initially identified in networks of phase oscillators with nonlocal coupling [1, 2], but they have been recently demonstrated for a wide range of oscillator networks [3]. This includes networks with couplings that have delays [4, 5], inertia [6, 7], time dependence or noise [8, 9], and are global [10, 11] or local [12–15]; it also includes networks of phase-amplitude oscillators [16, 17] and chaotic oscillators [18, 19]. Moreover, chimera states have been observed experimentally in various systems, including networks of optical [20], chemical [21], and mechanical [22] oscillators. Yet, with very few exceptions [23, 24], previous work has focused exclusively on chimeras in (discrete) network systems. It is thus natural to ask the extent to which chimeras states can exist and have salient properties in continuous systems.

We first note that continuum systems can exhibit analogous examples of coexisting order and disorder in homogenous media, but the connection between these phenomena and chimera states has remained largely unappreciated. Perhaps the most significant examples occur in fluid mechanics. Consider, for instance, a Taylor-Couette flow, where the fluid is constrained to the space between two rotating cylinders. As the rate of rotation increases the dynamics change from an orderly laminar regime to a turbulent one through a series of intermediate dynamical states [25], including a spiral turbulence flow regime characterized by a persistent spiraling region of turbulent flow which coexists with a domain of laminar flow [26]. The spiral turbulence in this system is thus a fluid counterpart of a chimera state. Related examples can be found in parametrically forced Faraday waves [27], where fluid driven by an oscillating support can form coexisting domains of regular stripes and chaotic surface waves, and in the spatiotemporal intermittency regime of Rayleigh-Bénard convection [28]. A key difference in continuous systems is in the nature of the coupling, which often consists of a strictly local (differential) component that acts in the limit of small spatial scales. Modeling chimera states in continuous systems and establishing that they can exist in the absence of any nonlocal coupling thus remains an important outstanding problem in this field. Although working directly with fluid equations is possible in principle, to address this problem it is more enlightening to employ simpler model equations.

In this Letter, we report on chimera states in the locally-coupled complex Ginzburg-Landau (CGL) equation in two spatial dimensions. These states, which we refer to as *frozen vortex chimeras*, correspond to coexisting domains of frozen spirals and amplitude turbulence and are characterized in a previously under-explored parameter regime of the system. They are distinct from spiral wave chimeras previously identified in discrete systems [29–31] in that the core of the spirals is coherent and the media lose coherence far from the core, and not the other way around. We analyze these states by introducing a local coupling field generalization of the Kuramoto-Battogtokh approach [1]. Crucially, we show that fluctuations in the coupling field cannot be neglected for such locally coupled continuous systems, which set them fundamentally apart from previously studied network analogs.

In the study of pattern formation, the CGL equation

$$\frac{\partial A}{\partial t} = A + (1 + ic_1)\nabla^2 A - (1 - ic_3)|A|^2 A \qquad (1)$$

describes the universal behavior of a homogenous oscil-

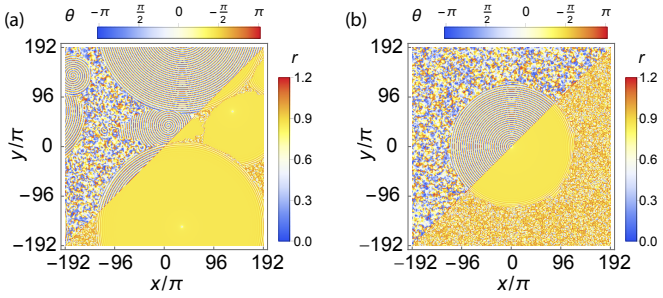

FIG. 1. Coexistence of coherent spirals and amplitude turbulence in the CGL system (1): (a) with $c_1 = 1.5$ and $c_3 = 0.77$ and random initial conditions after a time $t = 10^4$; (b) with $c_1 = 2.0$ and $c_3 = 0.85$ and a spiral initial condition after a time $t = 10^4$. The phase $\theta \equiv \arg(A)$ is depicted in the upper left and the amplitude $r \equiv |A|$ in the lower right.

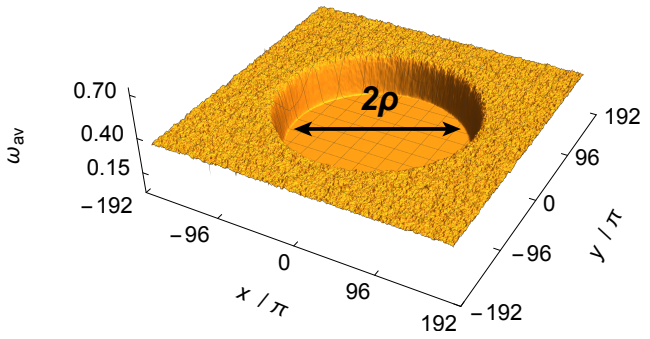

FIG. 2. Time-averaged angular frequency $\omega_{av} \equiv \langle \frac{d\theta}{dt} \rangle$ for the frozen vortex chimera in Fig. 1(b), where the arrow indicates the diameter 2ρ of the coherent region. The mean frequency in the coherent region is around 0.15, while the frequency is significantly higher (> 0.40) in the incoherent region. The distinction between the regions does not depend sensitively on the averaging interval (here taken to be $0 < t < 10^4$). For an animation of the time evolution of this chimera state, see Supplemental Material [47].

latory medium in the vicinity of a supercritical Hopf bifurcation; modeling applications of this equation include examples of Rayleigh-Bénard convection [32–34] and the Belousov-Zhabotinsky (BZ) reaction [35, 36]. The CGL system can exhibit a variety of dynamical phases depending on the parameters c_1 and c_3 [37]. As in other nonlinear wave systems [38], these phases include different coherent and localized structures. The most disordered phase is that of amplitude or defect turbulence, with a disordered and finite density of defects where $|A|$ reaches zero (and the phase of A is undefined) at a point. A second important phase consists of frozen spiral structures, where $|A|$ becomes time-independent near the spiral core and the phase of A has periodic spiraling structures. In particular, states with slowly evolving domains of frozen spirals, so-called vortex glass states, have attracted significant attention [39–42]. One relevant parameter regime previously studied corresponds to $c_1 = 2.0$ and $c_3 < 0.75$, in which the frozen (anti)-spirals [43] can nucleate out of amplitude turbulence and grow to a limited size [45]. Of special interest to our research question would be a parameter regime that supports frozen spiral states in a turbulent sea but with no growth and no spiral nucleation over relevant timescales.

Figure 1 shows results of our simulations of the CGL system (1). A regime in which coherent spirals have nucleated out of the amplitude turbulence and grown to their maximum size, with patches of residual amplitude turbulence between them, is shown in Fig. 1(a). As c_1 and c_3 are increased, on the other hand, the average time $T_{\rm nuc}$ required for spiral nucleation in a simulation area L^2 starting from an initial state of full amplitude turbulence rises sharply. For $c_1 = 2.0$ and $c_3 = 0.85$, for example, no spirals nucleate out of initial amplitude turbulence for times up to $t = 10^6$ (as verified for ten different simulation runs). However, spirals and amplitude turbulence do still coexist in this new regime; Fig. 1(b) shows a frozen vortex chimera after $t = 10^4$, which was obtain with an initial condition consisting of a single spiral that nucleated for smaller c_3. These numerical simulations are discrete approximations of the continuous CGL system of interest. In all simulations the system is taken to have linear size $L = 384\pi$ and is integrated using a pseudospectral algorithm with $N = 1536$ modes in each dimension [46]. We carried out a detailed study of these results with increasingly finer spatial grids and time steps (see Supplemental Material, Sec. S1 [47]). Crucially, we employ everywhere sufficiently fine spatial grids and time steps to ensure convergence to the continuum limit. These long-lived spatiotemporal patterns are *continuous-media chimera states* exhibiting a sizable coherent region (the spiral) and a sizable incoherent region (the amplitude turbulence phase).

Figure 2 shows the time-averaged frequency as a function of position in a frozen vortex chimera with $c_1 = 2.0$ and $c_3 = 0.85$. At the center there is a coherent domain, which is a frozen spiral of radius ρ with low mean angular frequency Ω, whereas the outer domain is occupied by an incoherent region, which has higher mean frequency and exhibits amplitude turbulence. The quantities ρ and Ω establish the natural length and time scales of the spiral. *We then formally define a frozen vortex chimera as a state in which there exists a spiral (of area $\pi\rho^2$) and a surrounding neighborhood of amplitude turbulence (of area comparable to $\pi\rho^2$) that persists without change for a time interval much longer than the spiral oscillation period of $2\pi/\Omega$.*

We now consider the parameter range over which such frozen vortex chimeras exist as both c_3 and c_1 are varied. These chimeras are intermediate states between the vortex glass phase and the amplitude turbulence phase, as shown in Fig. 3(a). We first note that if a spiral

is to coexist with amplitude turbulence for many periods of oscillation and qualify as a chimera, then: 1) the spiral must persists in its environment (which sets the boundary with the amplitude turbulence phase) and 2) rate of spiral nucleation in its neighborhood must be small compared to its angular frequency Ω (which sets the boundary with the vortex glass phase). To quantify the vortex glass transition, we define $\eta \equiv \frac{L^2}{\pi\rho^2}\frac{T_{\rm nuc}}{2\pi/\Omega}$, which is the nucleation time $T_{\rm nuc}$ properly normalized by the spiral period $2\pi/\Omega$ and the normalized neighborhood area $\pi\rho^2/L^2$. Our definition of a frozen vortex chimera requires $\eta \gg 1$, while states with faster spiral nucleation, and hence smaller η, are considered a vortex glass. Systematic simulations along the line $c_1 = 2.0$ revealed that frozen vortex chimeras exist up to values of $c_3 \lesssim 0.86$. Figure 3(b) shows a log-log plot of the normalized nucleation time η versus $0.86 - c_3$ for $c_1 = 2.0$. The transition boundary between vortex glasses and frozen vortex chimeras thus does not depend sensitively on the threshold for η, since the increase in η is extremely stiff as c_3 is increased, as demonstrated by the contour lines in Fig. 3(a) and the steep slope (approximately -10) in Fig. 3(b). Like other chimera states [48], frozen vortex chimeras are transient states. The mechanism of their collapse into coherent states is through the nucleation of new spirals in the neighborhood of the coherent domain. This process can take an exceedingly long amount of time. For example, the scaling in Fig. 3(b) suggests that the lifetime of the frozen vortex chimera in Fig. 2 is over a billion spiral oscillation periods.

It follows from Fig. 3(a) that the parameter regime where frozen vortex chimeras prevail is relevant for experimentally accessible systems such as the BZ reaction system [35, 36]. In models of the BZ system, the CGL parameter c_1 is determined primarily by species diffusion coefficients, while the parameter c_3 is determined by reaction rates and concentrations. By varying sulfuric acid concentrations, for example, the parameter regime $c_1 = 1.4$ and $0.5 < c_3 < 0.7$ just below the transition between vortex glasses and frozen vortex chimeras (around $c_3 \approx 0.8$ in Fig. 3) has been experimentally explored [36]. This provides evidence that frozen vortex chimeras can be realized experimentally in much the same fashion as in our numerical procedure. One important experimental consideration is the impact of imperfect experimental conditions—the basin of attraction of the frozen vortex chimeras must not be inaccessibly small if they are to be found in reality. To investigate this question, we have randomly perturbed the chimera state and observed its subsequent recovery or destruction (see Supplementary Materials, Sec. S2 [47]). So long as perturbations are not too large, the system is attracted back towards the frozen vortex chimera, thus providing evidence that with sufficiently controlled experimental conditions, frozen vortex chimeras should be experimentally accessible.

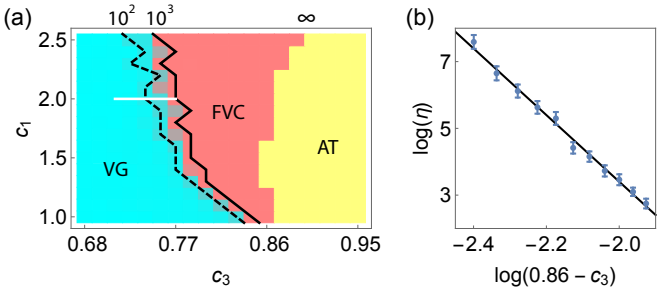

FIG. 3. (a) Diagram of dynamical phases of the CGL system, where the frozen vortex chimeras (FVC), vortex glass (VG), and amplitude turbulence (AT) occupy the intermediate, small, and large c_3 regions, respectively. The boundary between VG and FVC was determined by calculating η from five realizations of spiral nucleation from an amplitude turbulence initial state; the dashed line shows a modest change in this boundary as the threshold η changes by an order of magnitude around 10^3 (continuous line). The boundary between FVC and AT was determined by adiabatically varying c_1 and c_3 to move a spiral initial condition past the point of spiral destabilization. (b) Log-log plot of η for $c_1 = 2.0$ as a function of $0.86 - c_3$ corresponding to the white line in (a). Error bars show two times the standard deviation from 100 realizations, and the line marks the linear fit.

To analyze such chimera states, we employ a local coupling field approach similar to the one introduced in Ref. [1]. Local order parameters have also recently found application in the synchronization complex networks [49]. Rather than relying on the discrete local coupling fields used there, we derive the appropriate local coupling field in the continuous case of Eq. (1) by first differentiating $A = re^{i\theta}$ to obtain

$$\frac{\mathrm{d}\theta}{\mathrm{d}t} = \frac{1}{2i}\left(\frac{1}{A}\frac{\partial A}{\partial t} - \frac{1}{A^*}\frac{\partial A^*}{\partial t}\right), \tag{2}$$

where $*$ denotes complex conjugation. Using Eq. (1) in Eq. (2), we then identify the coupling terms as those involving spatial derivatives, namely $\frac{\sqrt{1+c_1^2}}{2ir}\left(\mathrm{e}^{i(\alpha-\theta)}\nabla^2 A - \mathrm{e}^{-i(\alpha-\theta)}\nabla^2 A^*\right)$, where $\alpha \equiv \arctan c_1$. To obtain evolution equations for r and θ analogous to those for discrete systems, it follows that the local coupling field should be defined as $Re^{i\Theta} \equiv \frac{\sqrt{1+c_1^2}}{r}\nabla^2 A$. Indeed, using this coupling field, Eq. (1) can be expressed as

$$\frac{\mathrm{d}\theta}{\mathrm{d}t} = c_3 r^2 + R\sin(\Theta - \theta + \alpha), \tag{3}$$

$$\frac{\mathrm{d}r}{\mathrm{d}t} = r(1 - r^2) + Rr\cos(\Theta - \theta + \alpha), \tag{4}$$

where the main difference from discrete phase oscillators is that the frequency term in the θ equation is a function of r and the coupling field is differential in r and θ.

Assuming a coupling field with time-independent $R(\mathbf{x})$ and $\Theta(\mathbf{x}, t) = \Omega t + \Phi(\mathbf{x})$ with Ω and $\Phi(\mathbf{x})$ time-independent, a coherent solution is one with $\mathrm{d}r/\mathrm{d}t = 0$

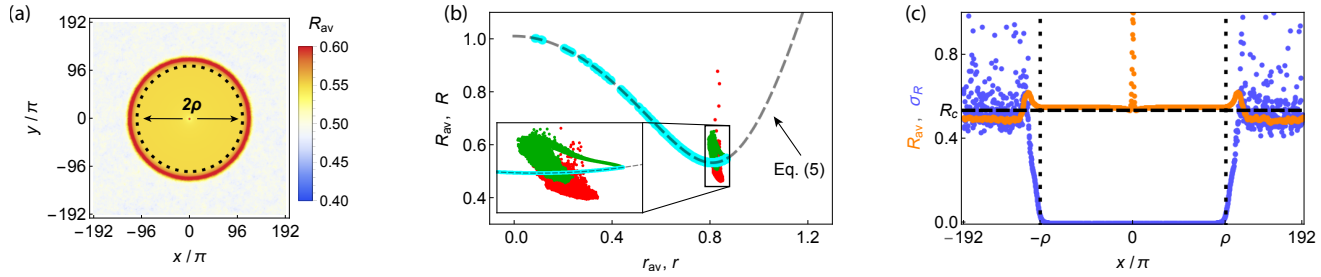

FIG. 4. (a) Time-averaged local coupling field R_{av} for the conditions in Fig. 2 as a function of: (a) the two spatial coordinates; (b) the time-averaged amplitude r_{av} for points in the coherent region (cyan dots), halo region (green dots), and remaining incoherent region (red dots); and (c) the x coordinate along the line $y = 0$ (orange dots). The inset in (b) magnifies the box, which includes all the points in the incoherent region. In (c) we also show the fluctuations σ_R of R (blue dots). The dotted lines in (a) and (c) delimitate the coherent domain in Fig. 2. The dashed lines in (b) mark the solution of Eq. (5) and in (c) mark the critical value $R = R_c$ above which Eq. (5) has (real) solutions.

and $\mathrm{d}\theta/\mathrm{d}t = \Omega$. Noting that $R^2 = R^2\sin^2(\Theta - \theta + \alpha) + R^2\cos^2(\Theta - \theta + \alpha)$ and solving Eqs. (3)-(4) for the trigonometric functions, the coherent solutions must satisfy $R^2 = (c_3 r^2 - \Omega)^2 + (1 - r^2)^2$. The amplitudes of these coherent solutions are

$$r = \sqrt{\frac{1 + c_3\Omega \pm \sqrt{(1 + c_3^2)R^2 - (c_3 - \Omega)^2}}{1 + c_3^2}}, \qquad (5)$$

where, given that R is real and positive, the condition for a (real) solution to exist is $R \geq R_c \equiv \frac{|c_3 - \Omega|}{\sqrt{1+c_3^2}}$.

Figure 4(a) shows the time-averaged local coupling field R_{av} of a frozen vortex chimera. As with other chimera states considered in the literature, we see that the coupling field amplitude is sufficiently large in the coherent domain to induce synchronization while it is too small to do so in the incoherent domain (with the exception of the red halo region surrounding the coherent domain). Figure 4(b) shows R_{av} and the time-averaged amplitude r_{av}, where it is clear that the solutions to Eq. (5) (dashed lines) correspond to the coherent domain (cyan dots). Note, however, that a portion of the desynchronized domain (green dots) has R_{av} larger (not smaller) than the corresponding solutions of Eq. (5), i.e., it satisfies $R_{av} > R_c = 0.54$. This portion corresponds to the red halo surrounding the coherent domain in Fig. 4(a). To understand why this halo region does not synchronize with the coherent domain, we must consider the fluctuations of the local coupling field. These fluctuations are quantified as the standard deviation σ_R calculated over the time series of R and are shown in Fig. 4(c).

A distinguishing property of the frozen vortex chimeras apparent in Fig. 4(c) is that, while negligible in the coherent domain, the fluctuations of the local coupling field rise in the halo region and saturate to large values in the amplitude turbulent domain. In the discrete nonlocal coupling scenario considered in the original formulation of the self-consistent mean-field approach [1], where many oscillators contribute to the mean field (in fact all of those for which the coupling kernel is not small), fluctuations in the mean-field solution are negligible in both the coherent *and* the incoherent domains. Incidentally, this underlies the increasing stability of chimera states with increasing system size in discrete network systems [48], rendering the thermodynamic limit of such systems sharply different from the continuous problem considered here. We argue that the origin of the difference in the nature of the fluctuations derives from the fact that the CGL system (1) is continuous and the coupling is local. Thus, the portion of the medium contributing to the local coupling field is not large enough to average out fluctuations.

We propose that the loss of synchrony across the halo region is driven by these enhanced fluctuations. The media in the halo is inclined to synchronize with the spiral because of the large local coupling field, but the large fluctuations present in the amplitude turbulent domain diffuse into the halo region and frequently disrupt this synchronization. A balance is achieved in which the inner spiral is shielded from the fluctuations in the amplitude turbulent domain by the halo, where the fluctuations decay and synchronization is repeatedly achieved and lost. To test this mechanism, we performed systematic simulations in which we directly modulate the fluctuations in the amplitude turbulent portion of the media (see Supplemental Materials, Sec. S3 [47]). Increasing the scale of the fluctuations causes the spiral to shrink in size, while decreasing them causes the spiral to grow. These simulations thus support the proposed fluctuation-based mechanism limiting the growth of the coherent spiral.

In summary, we have studied a novel chimera state appearing in the continuous locally-coupled complex Ginzburg-Landau equation. We noted that the nucleation of spiral structures out of an amplitude turbulent domain becomes negligibly small for a range of intermediate values of the parameter c_3, and thus that the chimeras persist without change for long times. In contrast to the fluctuations in chimera states in nonlocally coupled dis-

crete systems, fluctuations in the local coupling field in these chimera states cannot be neglected [50]. We conjecture that such fluctuations are responsible for the breakdown of coherence at the boundary between the coherent and incoherent domains. This appears to reflect a fundamental difference between the mechanism underlying the chimeras investigated here and those considered previously in nonlocal variants of the CGL equation [51]. This mechanism provides insights into experimental observations of coexisting order and disorder in continuous fluid media.

The authors acknowledge insightful discussions concerning theoretical aspects of continuous chimera states with Matthias Wolfrum and Jean-Régis Angilella and experimental aspects of the BZ system with Oliver Steinbock and Seth Fraden. This work was supported by ARO Award No. W911NF-15-1-0272 and NSF Award No. NSF-CMMI-1435358.

[1] Y. Kuramoto and D. Battogtokh, Nonlinear Phenom. Complex Syst. **5**, 380 (2002).
[2] D. M. Abrams and S. H. Strogatz, Phys. Rev. Lett. **93**, 174102 (2004).
[3] M. J. Panaggio and D. M. Abrams, Nonlinearity **28**, R67 (2015).
[4] J. H. Sheeba, V. K. Chandrasekar, and M. Lakshmanan, Phys. Rev. E **81**, 046203 (2010).
[5] L. Larger, B. Penkovsky, and Y. Maistrenko, Phys. Rev. Lett. **111**, 054103 (2013).
[6] T. Bountis, V. G. Kanas, J. Hizanidis, and A. Bezerianos, Eur. Phys. J. Spec. Top. **223**, 721 (2014).
[7] S. Olmi, Chaos **25**, 123125 (2015).
[8] A. Buscarino, M. Frasca, L. V. Gambuzza, and P. Hövel, Phys. Rev. E **91**, 022817 (2015).
[9] S. A. M. Loos, J. C. Claussen, E. Schöll, and A. Zakharova, Phys. Rev. E **93**, 012209 (2016).
[10] A. Yeldesbay, A. Pikovsky, and M. Rosenblum, Phys. Rev. Lett. **112**, 144103 (2014).
[11] G. C. Sethia and A. Sen, Phys. Rev. Lett. **112**, 144101 (2014).
[12] C. R. Laing, Phys. Rev. E **92**, 050904 (2015).
[13] B. K. Bera and D. Ghosh, Phys. Rev. E **93**, 052223 (2016).
[14] M. G. Clerc, S. Coulibaly, M. A. Ferré, M. A. García-Ñustes, and R. G. Rojas, Phys. Rev. E **93**, 052204 (2016).
[15] B. W. Li and H. Dierckx, Phys. Rev. E **93**, 020202 (2016).
[16] G. Bordyugov, A. Pikovsky, and M. Rosenblum, Phys. Rev. E **82**, 035205 (2010).
[17] G. C. Sethia, A. Sen, and G. L. Johnston, Phys. Rev. E **88**, 042917 (2013).
[18] I. Omelchenko, Y. Maistrenko, P. Hövel, and E. Schöll, Phys. Rev. Lett. **106**, 234102 (2011).
[19] C. Gu, G. St-Yves, and J. Davidsen, Phys. Rev. Lett. **111**, 134101 (2013).
[20] A. M. Hagerstrom, T. E. Murphy, R. Roy, P. Hövel, I. Omelchenko, and E. Schöll, Nat. Phys. **8**, 658 (2012).
[21] M. R. Tinsley, S. Nkomo, and K. Showalter, Nat. Phys. **8**, 662 (2012).
[22] E. A. Martens, S. Thutupalli, A. Fourrière, and O. Hallatschek, Proc. Natl. Acad. Sci. U.S.A. **110**, 10563 (2013).
[23] P. S. Skardal and J. G. Restrepo, Chaos **24**, 043126 (2014).
[24] L. Schmidt, K. Schönleber, K. Krischer, and V. García-Morales, Chaos **24**, 013102 (2014).
[25] C. D. Andereck, S. S. Liu, and H. L. Swinney, J. Fluid Mech. **164**, 155 (1986).
[26] J. J. Hegseth, C. D. Andereck, F. Hayot, and Y. Pomeau, Phys. Rev. Lett. **62**, 257 (1989).
[27] A. Kudrolli and J. P. Gollub, Physica D **97**, 133 (1996).
[28] S. Ciliberto and P. Bigazzi, Phys. Rev. Lett. **60**, 286 (1988).
[29] E. A. Martens, C. R. Laing, and S. H. Strogatz, Phys. Rev. Lett. **104**, 044101 (2010).
[30] O. E. Omel'chenko, M. Wolfrum, S. Yanchuk, Y. L. Maistrenko, and O. Sudakov, Phys. Rev. E **85**, 036210 (2012).
[31] M. J. Panaggio and D. M. Abrams, Phys. Rev. E **91**, 022909 (2015).
[32] M. C. Cross and P. C. Hohenberg, Rev. Mod. Phys. **65**, 851 (1993).
[33] Y. Liu and R. E. Ecke, Phys. Rev. Lett. **78**, 4391 (1997).
[34] S. Madruga, H. Riecke, and W. Pesch, Phys. Rev. Lett. **96**, 074501 (2006).
[35] L. Kramer, F. Hynne, P. Graae Sørenson, and D. Walgraef, Chaos **4**, 443 (1994).
[36] Q. Ouyang and J. M. Flesselles, Nature **379**, 143 (1996).
[37] I. S. Aranson and L. Kramer, Rev. Mod. Phys. **74**, 99 (2002).
[38] D. K. Campbell, in *AIP Conference Proceedings*, Vol. 376 (AIP, 1996) p. 115.
[39] G. Huber, P. Alstrøm, and T. Bohr, Phys. Rev. Lett. **69**, 2380 (1992).
[40] I. S. Aranson, L. Aranson, L. Kramer, and A. Weber, Phys. Rev. A **46**, R2992 (1992).
[41] C. Brito, I. S. Aranson, and H. Chaté, Phys. Rev. Lett. **90**, 068301 (2003).
[42] P. G. Kevrekidis, A. R. Bishop, and K. Ø. Rasmussen, Phys. Rev. E **65**, 016122 (2001).
[43] Anti-spirals are characterized by exhibiting inward rotation with a phase velocity that points towards the spiral core [44]. Here, we omit the prefix and refer to these structures simply as spirals.
[44] Y. Gong and D. J. Christini, Phys. Rev. Lett. **90**, 088302 (2003).
[45] H. Chaté and P. Manneville, Physica A **224**, 348 (1996).
[46] Our pseudospectral code is available at the repository `http://github.com/znicolaou/pseudospectral_cgl/`.
[47] See Supplemental Material for further analyses, illustrations, and details.
[48] M. Wolfrum and O. E. Omel'chenko, Phys. Rev. E **84**, 015201 (2011).
[49] A. Arenas, A. Díaz-Guilera, J. Kurths, Y. Moreno, and C. Zhou, Phys. Rep. **469**, 93 (2008).
[50] It is an open question as to whether analogous fluctuations are essential in the locally coupled discrete chimera states recently reported [12–15].
[51] L. Schmidt and K. Krischer, Chaos **25**, 064401 (2015).